



A Bidirectional FSO Communication Employing Phase Modulation Scheme and Remotely Injection-Locked DFB LD

Xu-Hong Huang , Chung-Yi Li, Hai-Han Lu , Senior Member, IEEE, Cing-Ru Chou, Hsin-Mao Hsia, and Yi-Hao Chen

Abstract—A bidirectional free-space optical (FSO) communication through a 600-m free-space transmission is built, employing a phase modulation (PM) scheme and a remotely injection-locked distributed feedback laser diode (DFB LD) for presentation. With optimum injection locking, a DFB LD is excellent for duplex transceiver operations. An injection-locked DFB LD not only operates as a PM-to-intensity modulation converter with an optical detector, but also functions as an upstream optical carrier. To be the first one of employing a remotely injection-locked DFB LD to detect a phase-modulated 25-Gb/s/25-GHz four-level pulse amplitude modulation (PAM4) passband signal, the DFB LD with remote injection locking is successfully intensity-modulated with an upstream 25-Gb/s non-return-to-zero (NRZ) signal. Good bit error rate performance and clear PAM4/NRZ eye diagrams show that this FSO communication can use a remotely injection-locked DFB LD to detect the downstream phase-modulated PAM4 signal and concurrently deliver an upstream intensity-modulated NRZ signal. This bidirectional 25-Gb/s/25-GHz (downstream)/25-Gb/s (upstream) FSO communication is prominent due to its enhancement in two-way high-speed optical wireless communications.

Index Terms—Four-level pulse amplitude modulation (PAM4), free-space optical (FSO) communication, phase modulation, remotely injection-locked DFB LD.

I. INTRODUCTION

WIRELESS broadband access (WBA) is attractive for supplying present and emerging technologies such as high-speed Internet, virtual/augmented reality, 4K/8K high-definition video transmission, and 5G/6G mobile telecommunication [1]–[6]. However, its low radio-frequency (RF) power feature limits

Manuscript received April 23, 2020; revised June 16, 2020; accepted June 26, 2020. Date of publication June 29, 2020; date of current version November 1, 2020. This work was supported in part by the Academia Collaboration from the National Taipei University of Technology (NTUT) and in part by National Taipei University (NTPU), under Grant USTP-NTUT-NTPU-109-01. (Corresponding author: Hai-Han Lu.)

Xu-Hong Huang is with the School of Information Science and Engineering, Fujian University of Technology, Fujian 350118, China (e-mail: huangxuh1@163.com).

Chung-Yi Li is with the Department of Communication Engineering, National Taipei University, New Taipei City 23741, Taiwan (e-mail: cyli@mail.ntpu.edu.tw).

Hai-Han Lu, Cing-Ru Chou, Hsin-Mao Hsia, and Yi-Hao Chen are with the Institute of Electro-Optical Engineering, National Taipei University of Technology, Taipei 10608, Taiwan (e-mail: hllu@ntut.edu.tw; b788949994@gmail.com; juson544938123@gmail.com; andy8804666@gmail.com).

Color versions of one or more of the figures in this article are available online at <https://ieeexplore.ieee.org>.

Digital Object Identifier 10.1109/JLT.2020.3005714

its wireless access distance. Modern access, metro, and long-haul core networks need increased transmission capacity to cover Internet, 5G/6G mobile telecommunication, and cloud computing applications. Increasing demands are pushing the requirements of long-range wireless access and high transmission capacity. Following optical wireless communication technology's evolution, free-space optical (FSO) communication has attracted substantial attention because of its numerous benefits over RF-based WBA, such as unlicensed bandwidth, non-interference with RF signals, and affording an optical wireless link in certain area in which RF wireless link is restricted. Compared with RF-based WBA, FSO communication is enhanced with free-space link of hundreds of meters and data rate of tens of gigabits [7]–[12]. The performance of FSO communications will be subject to bad weather. Atmospheric turbulence because of thick fog or heavy rain will affect FSO communication's link availability and bring on poor performance. In the scenario of thick fog or heavy rain, however, millimeter-wave (MMW) link can be deployed as a substitute solution [13]. As for the eye safety problem of FSO communications, people have a natural aversion to laser light and are liable to turn their heads or close their eyes if exposed, meaning that people will not stare at the laser light due to natural reaction. Thus, the risk of eye damage can be alleviated since people's natural reaction makes it difficult to expose the eyes over a long time.

Phase-modulated FSO communication requires a costly delay interferometer (DI) [14] or a sophisticated fiber Bragg grating (FBG) tilt filter [15], [16] to convert the phase-modulated optical signal into an intensity-modulated signal before being sent to a photodiode (PD). However, a costly DI or sophisticated FBG tilt filter will severely restrict the constructing of phase-modulated FSO communication. Developing an inexpensive and unsophisticated phase modulation (PM)-to-intensity modulation (IM) converter is thus imperative for constructing a phase-modulated FSO communication. To conquer the restriction of costly DI or sophisticated FBG tilt filter, a distributed feedback laser diode (DFB LD) with remote injection locking is thereby offered to make a PM-to-IM conversion. Gu *et al.* [17] and Su *et al.* [18] experimentally employed an injection-locked vertical-cavity surface-emitting laser (VCSEL) or DFB LD to directly detect phase-modulated optical signal. Experiments have shown that as a VCSEL or DFB LD is remotely injection-locked, a phase-modulated optical signal can be converted to

an intensity-modulated signal. In addition, an electrical signal can be acquired from the electrical port of an injection-locked VCSEL or DFB LD. An injection-locked VCSEL was used to directly detect phase-modulated 12-Gb/s non-return-to-zero (NRZ) baseband signal in a digital fiber optics transmission system [17], and an injection-locked DFB LD was used to directly detect phase-modulated 50–550 MHz analog CATV signal in a fiber optical CATV transmission system [18]. Nevertheless, applying it to detect phase-modulated PAM4 passband signal in a bidirectional FSO communication has not been addressed. In this study, a bidirectional FSO communication with a downstream phase-modulated 25-Gb/s/25-GHz PAM4 passband signal and an upstream intensity-modulated 25-Gb/s NRZ baseband signal over a 600-m free-space transmission is proposed and constructed. Importantly, a bidirectional FSO communication, rather than a unidirectional FSO communication, must be built and implemented. One of the merits of FSO communications is to offer the spatial reuse. A bidirectional FSO communication that delivers symmetrical downstream and upstream transmission rates is thus built to meet the spatial reuse target. PAM4's data rate is twice that of NRZ at a given bandwidth, making PAM4 suitable for high-speed transmission [19]–[21]. Regarding PM scheme, it provides high robustness against noise since PM scheme utilizes phase shifting to write down signal states. In FSO communications, noise increases as other lights from the environment increase, by which bringing on link performance degradation. Compared with IM scheme, PM scheme can further enhance the link performance of FSO communications due to higher noise tolerance. Although a PM-to-IM converter is required at the receiving side, however, PM scheme is worth adopting because it has better link performance than IM scheme.

To successfully deploy a bidirectional FSO communication, an optical carrier is needed at the receiver side for upstream modulation. Wavelength reuse is commonly utilized in bidirectional lightwave transmission systems for upstream transmission. The feasibility of adopting a reflective semiconductor optical amplifier (RSOA) for wavelength reuse in bidirectional lightwave transmission systems was performed formerly [22]–[25]. Nevertheless, sending a 25-Gb/s NRZ data stream via an RSOA is quite challenging since RSOA's bandwidth is limited. A DFB LD with remote injection locking is a promising mechanism for upstream transmission. An injection-locked DFB LD's bandwidth is several times that of an RSOA. This allows FSO communication enhancing the upstream transmission capacity without using an electrical equalizer [26], [27]. In addition, the upstream performance for employing an injection-locked DFB LD is better than that for employing an RSOA, due to the reduction of laser chirp caused by direct modulation [28]. Consequently, a DFB LD with remote injection locking is a promising mechanism because it can not only function as a PM-to-IM converter with an optical detector to detect the phase-modulated optical signal, but it can also function as an upstream optical carrier to provide improved upstream performance. To the author's best knowledge, this is the first time that an injection-locked DFB LD is adopted to detect a downstream phase-modulated PAM4 passband signal and deliver an upstream intensity-modulated NRZ baseband

signal concurrently. With optimal injection wavelength and injection power, a remotely injection-locked DFB LD effectively operates as a duplex transceiver. Compared with previous works [17], [18], the realization of such a bidirectional FSO communication with phase-modulated 25-Gb/s/25-GHz PAM4 passband signal (downstream) and intensity-modulated 25-Gb/s NRZ baseband signal (upstream) is a challenge, especially for a 600-m long-range free-space transmission and given transmission qualities. It is difficult to obtain good transmission performances due to high downstream/upstream transmission rates and long-reach free-space transmission. Employing an injection-locked DFB LD to detect downstream phase-modulated 25-Gb/s/25-GHz PAM4 passband signal and transmit upstream intensity-modulated 25-Gb/s NRZ baseband signal in a bidirectional FSO communication is more difficult than employing an injection-locked VCSEL (DFB LD) to detect downstream phase-modulated 12-Gb/s NRZ baseband signal (50–550 MHz analog CATV signal) and transmit upstream intensity-modulated 12-Gb/s NRZ baseband signal (50–550 MHz analog CATV signal) in a bidirectional fiber optics transmission system. Furthermore, laser light alignment is imperative for a bidirectional FSO communication. Thanks to strict laser light alignment requirement, it is quite challenging for a bidirectional FSO communication to maintain the link availability. To ensure a practical operation of bidirectional FSO communication through 600 m free-space transmission, these technique challenges must be conquered [29].

The link performances of the demonstrated bidirectional FSO communication through 600 m free-space transmission are investigated in real-time via bit error rate (BER) values and PAM4/NRZ eye diagrams. Good BER performances and clear PAM4/NRZ eye diagrams are attained over a 600-m free-space link. This bidirectional 25-Gb/s/25-GHz (downstream)/25-Gb/s (upstream) FSO communication with low-complexity duplex transceiver opens up a novel and promising way for developing two-way high-speed optical wireless communications.

II. EXPERIMENTAL SETUP

Fig. 1 presents two bidirectional FSO communications employing downstream phase-modulated 25-Gb/s/25-GHz PAM4 passband signal and upstream intensity-modulated 25-Gb/s NRZ baseband signal over 600 m free-space transmission. Fig. 1(a), denoting system I, illustrates an FSO communication employing an FBG tilt filter with a PD at the receiving side. Fig. 1(b), denoting system II, illustrates our proposed FSO communication's framework which employs a remotely injection-locked DFB LD as a duplex transceiver. DFB LD1, with a central wavelength of 1540.60 nm (λ_1), inputs an optical carrier into the phase modulator (Thorlabs LN66S) after being polarized by a polarization controller (PC1). A 25-Gb/s PAM4 baseband signal generated from a PAM4 signal generator (Anritsu MP1800A), with an amplitude of 1.2 V_{pp}, is mixed with a 25-GHz MMW carrier to produce a 25-Gb/s/25-GHz PAM4 passband signal. Since PAM4's linearity is imperative, a passive linear equalizer (Anritsu J1646A) is employed to drive the PAM4 electrical signal. A mixer (HMC337), with frequency

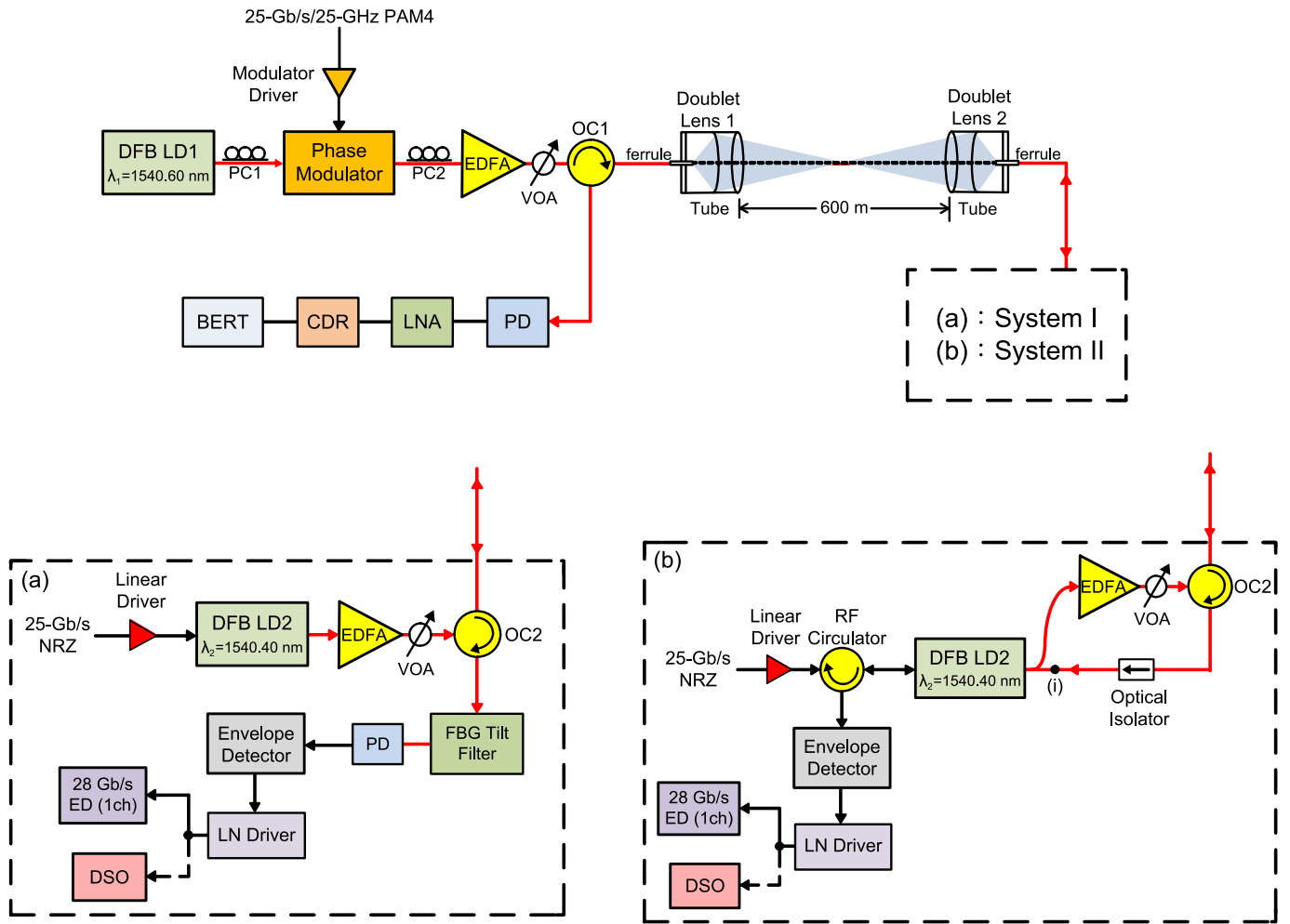


Fig. 1. Two bidirectional FSO communications employing a downstream phase-modulated 25-Gb/s/25-GHz PAM4 passband signal and an upstream intensity-modulated 25-Gb/s NRZ baseband signal through a 600-m free-space transmission.

range of 17–25 GHz/maximum local oscillator input power of 13 dBm/maximum RF output power of 13 dBm, is utilized to mix the PAM4 signal with the 25 GHz carrier. After traveling through a modulator driver, this 25-Gb/s/25-GHz PAM4 passband signal is supplied in the phase modulator with a half-wave voltage of 3.9 V at DC, 7 V at 1 GHz, and 10 V at 25 GHz. As the lightwave is modulated by a phase modulator, several sidebands will be produced depending on the amplitude of the driven PAM4 passband signal. We drive the phase modulator with 3.4% optical modulation index, by which resulting in only the first-order (± 1) sidebands are generated. The peak of first-order sidebands is 25 GHz away from the zero-order carrier. Then, a PC (PC2) is employed to adjust the optical signal’s polarization state. The 25-Gb/s/25-GHz PAM4 passband signal is boosted by an erbium-doped fiber amplifier (EDFA), decreased by a variable optical attenuator (VOA), circulated by an optical circulator (OC1), and communicated over 600 m free-space transmission via a set of doublet lenses. As EDFA’s input power is 0 dBm, its output power and noise figure are 17 dBm and 4.5 dB, respectively. A VOA after the EDFA optimizes the optical power sent to the free-space. Doublet lenses emit the laser light from

doublet lens 1 to the free-space and direct the laser light from the free-space to doublet lens 2. The downstream optical signal is sent to system I [Fig. 1(a)] and system II [Fig. 1(b)], respectively, over 600 m free-space transmission.

In system I, the downstream optical signal is circulated by an OC2, and then passed through an FBG tilt filter to perform a PM-to-IM conversion. Following with the FBG tilt filter, the optical signal is received by a broadband PD (Optilab PR-30-A) with 30 GHz bandwidth, and envelope-detected by an envelope detector with 0.5-43.5 GHz frequency range (Analog Devices ADL6010). After driven by a low-noise (LN) driver (Anritsu AH34152A), the 25-Gb/s PAM4 baseband signal experiences real-time BER measurement by a 28-Gb/s error detector (ED) (Anritsu MP1800A 28-Gb/s ED). Further, a digital storage oscilloscope (DSO) (Keysight N1000A DCA-X) catches the 25-Gb/s PAM4 signal’s eye diagrams.

For uplink transmission, a 25-Gb/s NRZ data stream is driven by a linear driver (Picosecond PSPL5866) and fed into the DFB LD2 ($\lambda_c = 1540.40$ nm). Next, the upstream optical signal is boosted by an EDFA, reduced by a VOA, circulated by an OC2, and transmitted through 600 m free-space link by

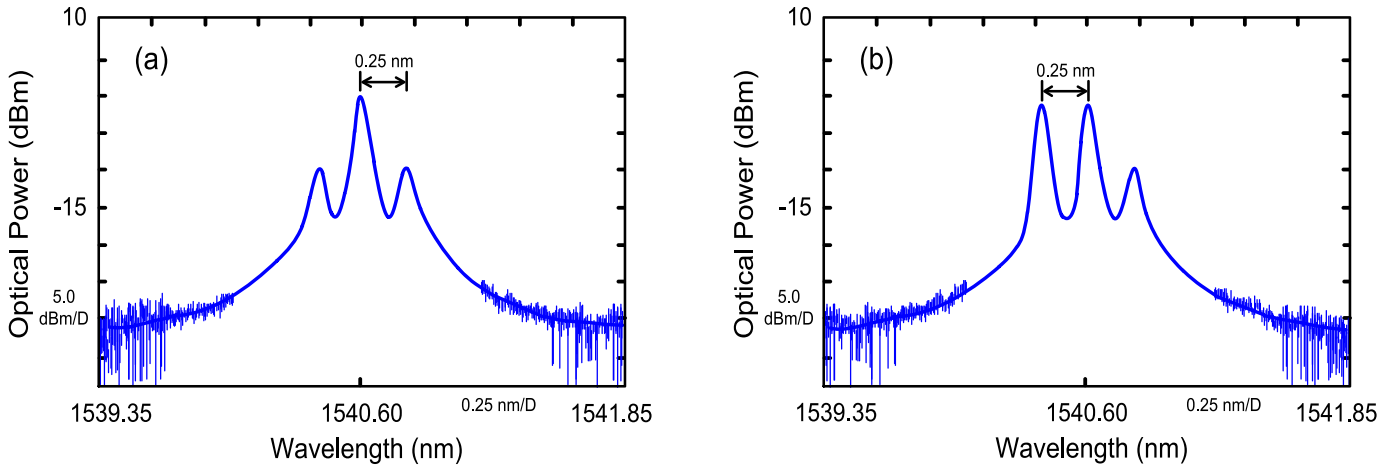


Fig. 2. (a) The optical spectrum before injection locking. (b) A remote injection locking will enhance the lower sideband's intensity.

a pair of doublet lenses. Subsequently, the upstream signal is circulated by an OC1, detected by a 25-GHz PD (Newport 1414), amplified by a 25-GHz low noise amplifier (LNA) (SHF 115 AP), recovered through a 25-Gb/s clock/data recovery (DSC-25G-CDR), and sent to a BER tester (BERT) (Anritsu MP2101A) to measure the BER.

In system II, the downstream optical signal is circulated by an OC2, travelled through an optical isolator, and injected into the DFB LD2 to operate a PM-to-IM conversion and detect a 25-Gb/s/25-GHz PAM4 passband signal. Given that the DFB LD2 is remotely injection-locked, the lower sideband (-1 sideband) of the phase-modulated optical signal is enhanced. Whereas the upper sideband ($+1$ sideband) remains unchanged. The optical spectrum before injection locking is shown in Fig. 2(a) [Fig. 1(b) insert (i)]. A remote injection locking will enhance the lower sideband's intensity and generate the optical spectrum as presented in Fig. 2(b). An optical isolator between the OC2 and DFB LD2 prevents the upstream optical signal from the injection-locked DFB LD2 to ensure it has been entirely delivered for uplink transmission. Afterward, the 25-Gb/s/25-GHz PAM4 passband signal is circulated by an RF circulator with a frequency range of 17.7–26.5 GHz (Wenteq F3796), envelope-detected by an envelope detector, and driven by a LN driver. Subsequently, a high-sensitivity ED measures the BER in real-time, and a DSO takes the 25-Gb/s PAM4 baseband signal's eye diagrams.

For uplink transmission, a 25-Gb/s NRZ data stream is driven by a linear driver, circulated by an RF circulator, and inputted into the injection-locked DFB LD2. Next, the upstream optical signal is boosted by an EDFA, controlled by a VOA, circulated by an OC2, and transported through 600 m free-space transmission via a couple of doublet lenses. Afterward, the upstream signal is circulated by an OC1, detected by a 25-GHz PD, amplified by a 25-GHz LNA, recovered through a 25-Gb/s CDR, and inputted into a BERT to evaluate the BER performance.

The setup for measuring the downstream/upstream modulation response of bidirectional FSO communications is presented in Fig. 3. For downstream modulation response, a continuous sweep signal (DC – 26 GHz) produced from a network analyzer

is supplied in the phase modulator. After detection by the DFB LD2 and circulation by an RF circulator, the sweep signal is returned to the network analyzer. Thereby, the downstream modulation response is measured in the scenarios of DFB LD2 with remote injection locking and non-injection locking. As for upstream modulation response, a continuous sweep signal (DC – 26 GHz) is circulated by an RF circulator, and then supplied in the free-running/injection-locked DFB LD2. After circulation by an OC1 and detection a PD, the sweep signal is returned to the network analyzer. Accordingly, the upstream modulation response is measured in the scenarios of DFB LD2 with free-running and injection locking.

III. EXPERIMENTAL RESULTS AND DISCUSSIONS

In this demonstration, a couple of doublet lenses emit and receive laser light over 600 m free-space link for building a bidirectional FSO communication. For indoor application, a 600-m free-space transmission with plane mirror on each corner can avoid the transmission interruption due to physical obstructions [2]. For outdoor application, a 600-m free-space transmission can meet the target of two building's communication [7]. As a laser light travels through a 600-m FSO link, the laser light's natural expansion [30] makes it difficult to totally couple the laser light with the fiber ferrule. Doublet lens at the receiving side is a reduction scheme to match the laser light with the fiber ferrule's field of view (FOV). If fiber ferrule's FOV is larger than doublet lens's FOV, as illustrated in Fig. 4(a), then fiber ferrule accumulates more transmitted laser light. Thus, the received optical power increases and improves the BER performance. Nevertheless, if doublet lens's FOV is larger than fiber ferrule's FOV, as illustrated in Fig. 4(b), then fiber ferrule accumulates less transmitted laser light. Thus, the received optical power decreases and worsens the BER performance.

Table I gives the status of the DFB LD2 with injection at different wavelength detuning ($\Delta\lambda = \lambda_1 - \lambda_2$). Notably, an injection locking behavior emerges within the wavelength detuning range of -0.2 to 0.3 nm. However, severe oscillation appears outside the wavelength detuning range [31], [32]. Within the

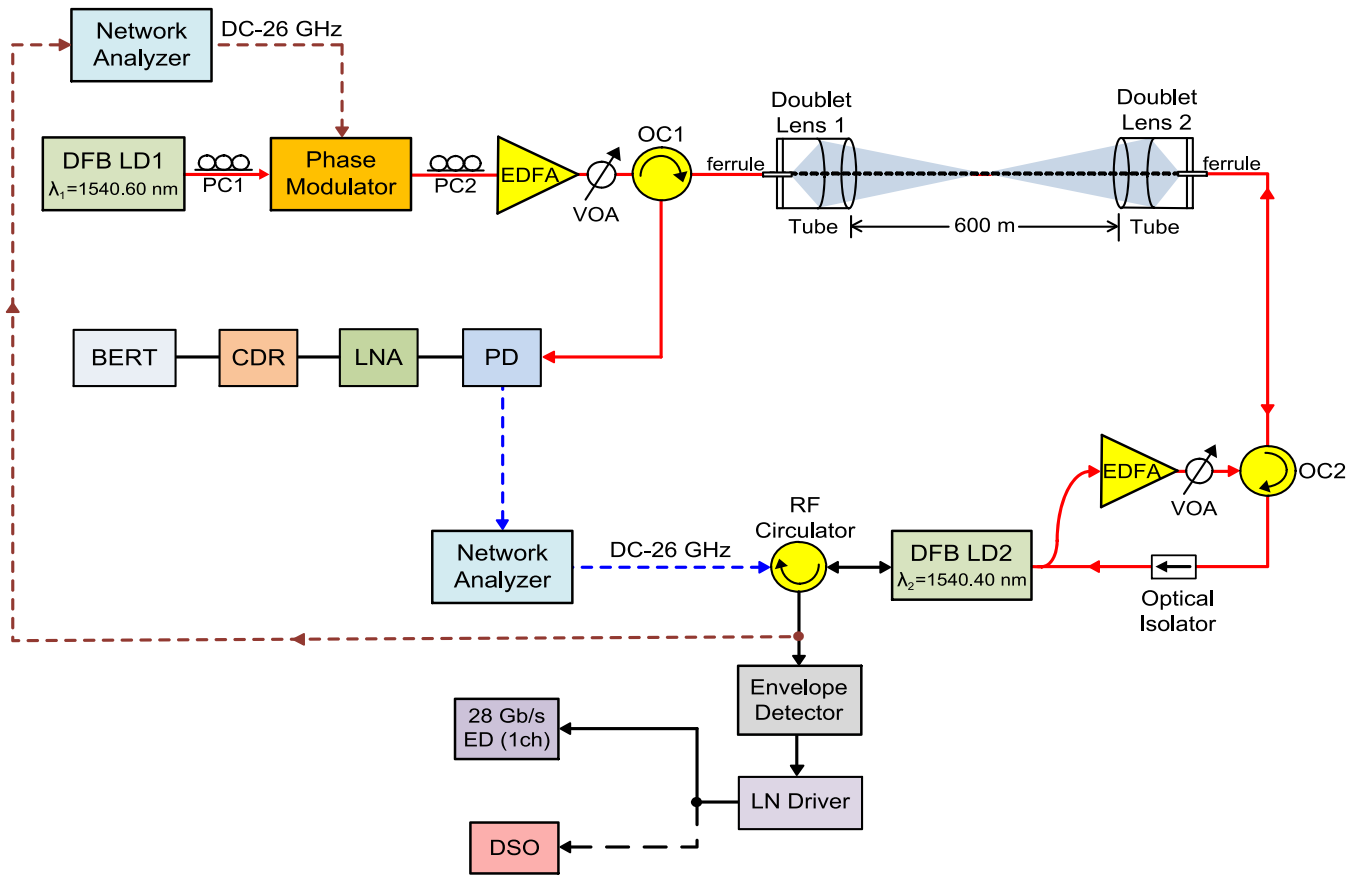


Fig. 3. The setup for measuring the downstream/upstream modulation response of bidirectional FSO communications.

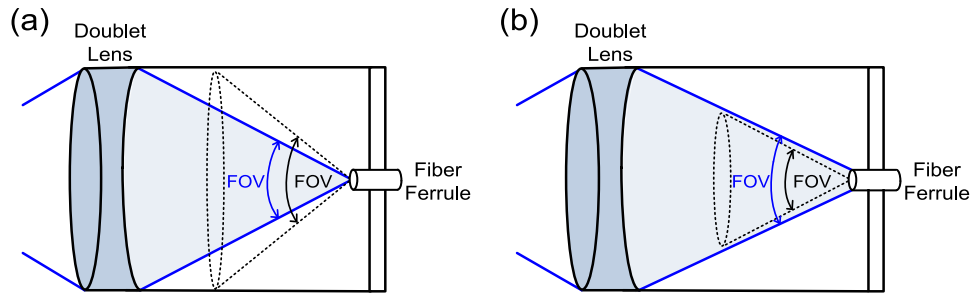


Fig. 4. (a) Fiber ferrule's FOV is larger than doublet lens's FOV. (b) Doublet lens's FOV is larger than fiber ferrule's FOV.

injection locking range, the DFB LD2 functions as a PM-to-IM converter with an optical detector. Outside the injection locking range, however, the DFB LD2 will not function as a PM-to-IM converter with an optical detector. Moreover, it is to be found that optimum injection locking occurs at a wavelength detuning of ± 0.2 nm. With optimum injection locking, this proposed bidirectional FSO communication performs best in view of the lowest BER value.

Fig. 5 shows the downstream/upstream modulation responses of bidirectional FSO communications in the conditions of DFB LD2 with injection locking and non-injection locking (downstream)/free-running (upstream). For downstream modulation, it is to be observed that only noise is attained as

the DFB LD2 has not injection-locked by the phase-modulated PAM4 passband signal. With injection locking, nevertheless, a great enhancement in resonance frequency and a considerable improvement in 3-dB modulation response are obtained. Result shows that DFB LD2 with injection locking is powerful for an optical detector to detect downstream 25-Gb/s/25-GHz PAM4 passband signal and an optical transmitter to transmit upstream 25-Gb/s NRZ baseband signal simultaneously. The downstream and upstream transmission rates can be further enhanced by employing a bidirectional FSO communication with a 3-dB modulation response higher than 25.4 GHz, indicating that they can be further increased by employing a remotely injection-locked DFB LD2 with a 3-dB resonance frequency

TABLE I
THE STATUS OF THE DFB LD2 WITH INJECTION AT DIFFERENT WAVELENGTH DETUNING ($\Delta\lambda = \lambda_1 - \lambda_2$).

$\Delta\lambda = \lambda_1 - \lambda_2$ (nm)	0.4	0.3	0.2	0.1	0	-0.1	-0.2	-0.3
Status	Severe Oscillation	Injection Locking	Injection Locking	Injection Locking	Injection Locking	Injection Locking	Injection Locking	Severe Oscillation

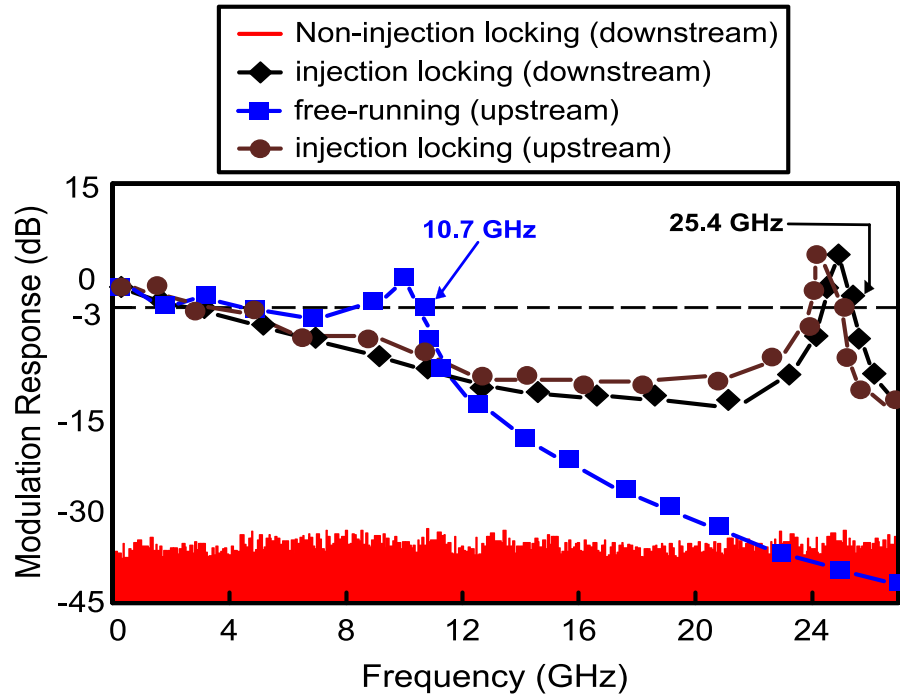


Fig. 5. The downstream/upstream modulation responses of bidirectional FSO communications in the conditions of DFB LD2 with injection locking and non-injection locking (downstream)/free-running (upstream).

(modulation response) higher than 25.4 GHz. If a downstream phase-modulated 50-Gb/s/25-GHz PAM4 passband signal and an upstream intensity-modulated 25-Gb/s PAM4 baseband signal are adopted, then there would be two PAM4 signal generators to build such a bidirectional FSO communication. In this manner, complexity and cost increase due to the use of two PAM4 signal generators for downlink and uplink transmissions. For a practical implementation of bidirectional FSO communication, it is vital to have a framework with simple and cost-effective advantages. Moreover, at a 10^{-9} BER operation, since the receiver sensitivity of 50-Gb/s PAM4 signal is higher than that of 25-Gb/s PAM4 signal, the power penalty in BER performance will be paid for the 50-Gb/s/25-GHz PAM4 passband signal. In addition, given that PAM4 is more susceptible to noise than NRZ, the upstream performance for delivering a 25-Gb/s PAM4 baseband signal will be worse than that for transmitting a 25-Gb/s NRZ baseband signal.

Fig. 6(a) shows the downstream BER performances of FSO communications with phase-modulated 25-Gb/s/25-GHz PAM4 passband signal in the states over 600-m FSO link (system I), over 600-m FSO link (system II; with 3 dBm injection), over

600-m FSO link (system II; with 0 dBm injection), and over 600-m FSO link (system II; with -3 dBm injection), respectively. Over 600-m FSO link, the atmospheric attenuation varies from 1.4 dB (good visibility) to 50 dB (poor visibility) [33]. In this study, an atmospheric attenuation of around 1.6 dB exists because of 600 m free-space transmission, a coupling loss of about 2.2 dB emerges due to laser light travelling through a couple of doublet lenses, a coupling loss of approximately 1.2 dB appears on account of laser light coupling into fiber ferrule (receiving side), and an insertion loss of around 1 dB happens as laser light passing through an OC2 with an optical isolator. Thereby, a link budget of 6 dB ($1.6 + 2.2 + 1.2 + 1$) exists. With a link budget of 6 dB and an injection power of 3 dBm, thus, the transmitted laser power at the doublet lens 1 is 9 dBm [$6 \text{ (dB)} + 3 \text{ (dBm)} = 9 \text{ (dBm)}$]. Although 9 dBm laser power is higher than the eye safety of laser power level regulation, however, the risk of eye damage can be avoided by erecting a couple of doublet lenses on two building's roofs (outdoor) and can be mitigated by transmitting laser light from the ceiling to the floor (indoor) to keep away from looking straight at the laser. At a BER value of 10^{-9} , there is a power penalty of approximately

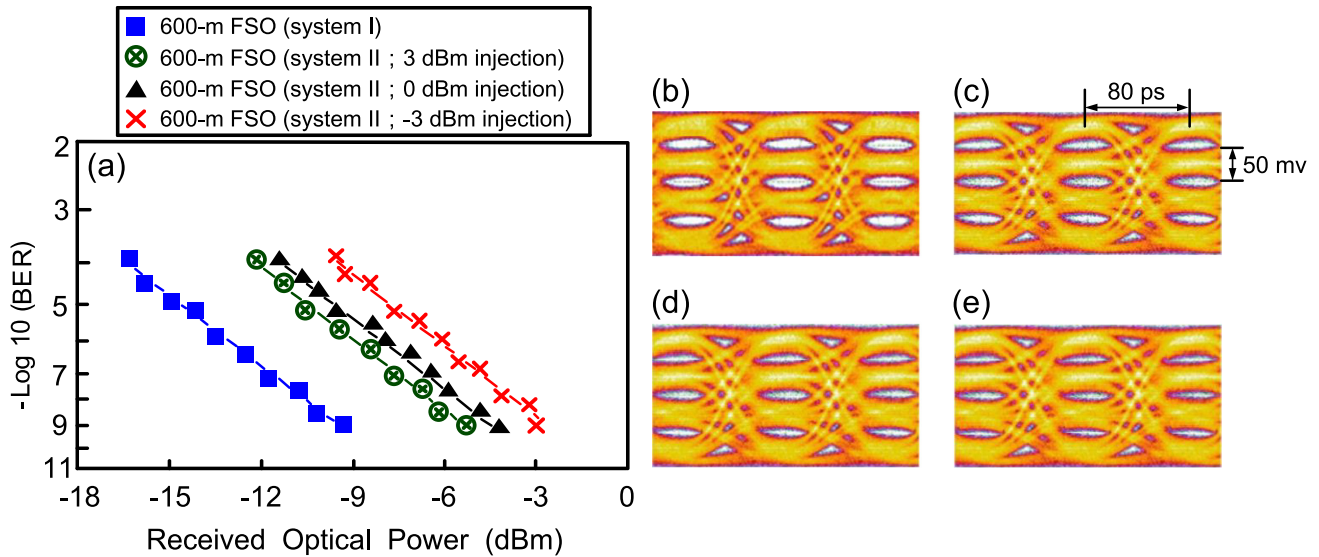


Fig. 6. (a) The downstream BER performances of FSO communications with phase-modulated 25-Gb/s/25-GHz PAM4 passband signal in the states over 600-m FSO link (system I), over 600-m FSO link (system II; with 3 dBm injection), over 600-m FSO link (system II; with 0 dBm injection), and over 600-m FSO link (system II; with -3 dBm injection). The eye diagrams of down-converted 25-Gb/s PAM4 signal delivered (b) over a 600-m FSO link (system I), (c) over a 600-m FSO link (system II; with 3 dBm injection), (d) over a 600-m FSO link (system II; with 0 dBm injection), and (e) over a 600-m FSO link (system II; with -3 dBm injection).

4.1 dB between systems I and II (with 3 dBm remote injection). To have the same BER performance for systems I and II (with 3 dBm injection), the received optical power of system I has to be decreased 4.1 dB (power penalty) to achieve the same BER performance. In system I, a BER value of 10^{-9} is attained at a received optical power of -9.3 dBm. In system II (with 3 dBm injection), therefore, a BER value of 10^{-9} is derived at a received optical power of -5.2 dBm. The 4.1-dB power penalty mainly results from the injection-locked DFB LD2's large dynamic nonlinearity at the resonance frequency [34]. As DFB LD2 is injection-locked, dynamic laser nonlinearity becomes large when the modulated frequency is closer to the resonance frequency. As modulated signal around the resonance frequency is utilized for PAM4 passband signal transmission, nonlinear distortion becomes large and thus worsens the BER performance. To avoid large dynamic laser nonlinearity (large nonlinear distortion), the modulated frequency must be lower than the resonance frequency of the injection-locked DFB LD2. Nevertheless, system II's (with 3 dBm injection) BER performance still meets the target of FSO communications ($\leq 10^{-9}$). Moreover, it is to be found that system II's BER performance is obviously influenced by the DFB LD2's injection power level. With a 10^{-9} BER operation, a 1-dB power penalty appears between the states over 600-m FSO link (system II; with 3 dBm injection) and that over 600-m FSO link (system II; with 0 dBm injection). At a BER value of 10^{-9} , a 1.1-dB power penalty occurs between the states over 600-m FSO link (system II; with 0 dBm injection) and that over 600-m FSO link (system II; with -3 dBm injection). It discloses the DFB LD2 with remote injection locking can practically function as a PM-to-IM converter with an optical detector. The conversion and detection efficiencies are proportional to the injection power

level. Remote injection locking with higher injection power level yields higher conversion and detection efficiencies, thus improving the downstream BER performance.

Figs. 6(b), 6(c), 6(d), and 6(e) display the eye diagrams of the down-converted 25-Gb/s PAM4 signal delivered over a 600-m FSO link (system I), over a 600-m FSO link (system II; with 3 dBm injection), over a 600-m FSO link (system II; with 0 dBm injection), and over a 600-m FSO link (system II; with -3 dBm injection), respectively. In the state over 600-m FSO link (system I), open eye diagrams [Fig. 6(b)] are attained with a BER operation of 10^{-9} and a received optical power of -9.3 dBm. In the state over 600-m FSO link (system II; with 3 dBm injection), clear eye diagrams [Fig. 6(c)] are observed at a BER value of 10^{-9} and a received optical power of -5.2 dBm. Over 600-m FSO link (system II; with 0 dBm injection), somewhat clear eye diagrams [Fig. 6(d)] are obtained with a BER operation of 10^{-9} and a received optical power of -4.2 dBm. Over 600-m FSO link (system II; with -3 dBm injection), a little worse than clear eye diagrams [Fig. 6(e)] are acquired at a BER value of 10^{-9} and a received optical power of -3.1 dBm.

Figs. 7(a), 7(b), and 7(c) exhibit the electrical spectra of the downstream 25-Gb/s PAM4 signal in the conditions over 600-m FSO link (system I), over 600-m FSO link (system II; with 3 dBm injection), and over 600-m FSO link (system II; non-injection locking), respectively. The PD (system I), the injection-locked DFB LD2 (system II; with 3 dBm injection), and the non-injection-locked DFB LD2 (system II; non-injection locking) are compared. Fig. 7(b) shows that an injection-locked DFB LD2 (system II; with 3 dBm injection) can detect the delivered 25-Gb/s PAM4 signal but with a lower amplitude in comparison with the PD (system I). The amplitude of the 25-Gb/s PAM4 signal detected by the injection-locked DFB LD2 (system II;

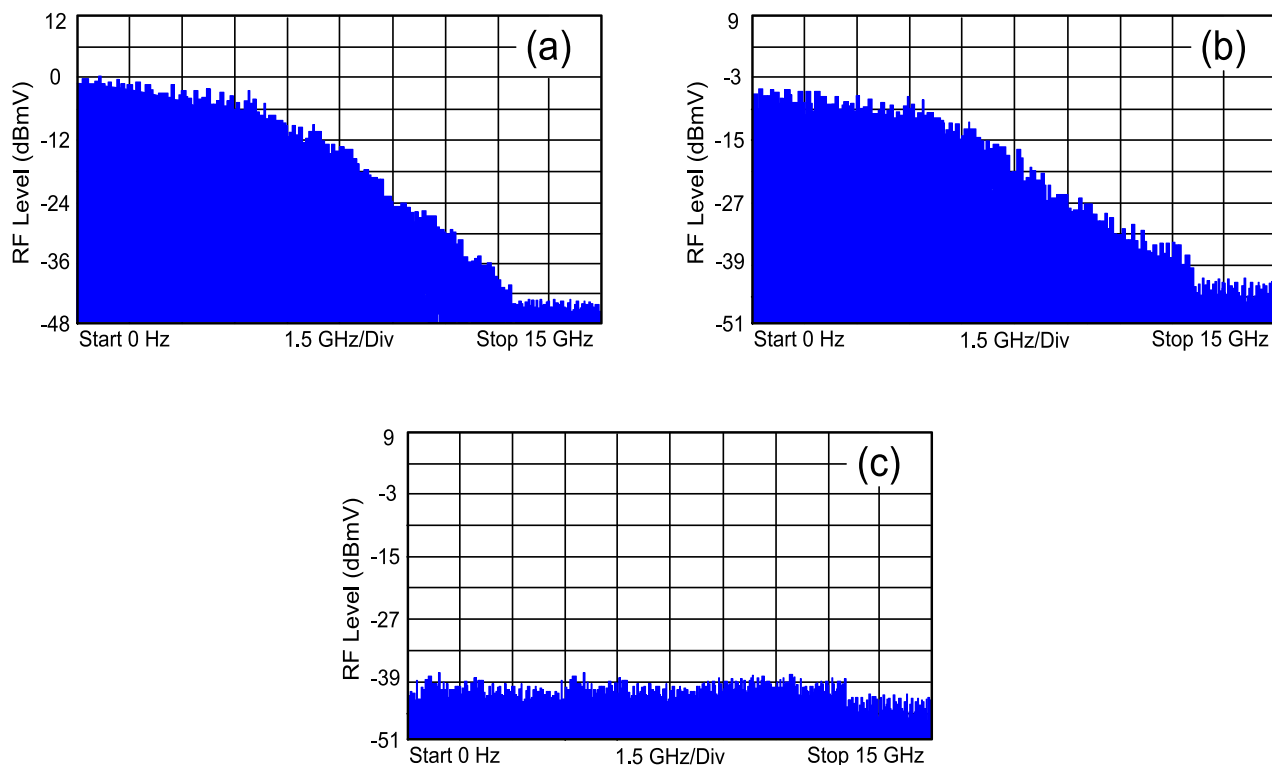


Fig. 7. Electrical spectra of the downstream 25-Gb/s PAM4 signal in the conditions (a) over 600-m FSO link (system I), (b) over 600-m FSO link (system II; with 3 dBm injection), and (c) over 600-m FSO link (system II; non-injection locking).

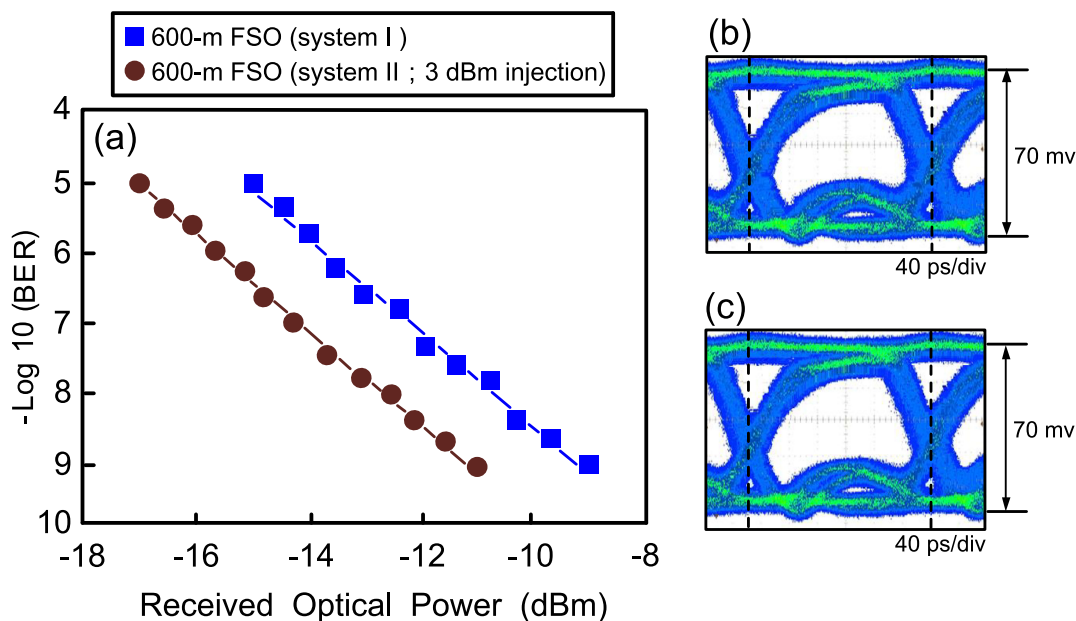


Fig. 8. (a) The upstream BER performances of FSO communications with intensity-modulated 25-Gb/s NRZ signal in the scenarios over 600-m FSO link (system I) and that over 600-m FSO link (system II; with 3 dBm injection). The delivered 10-Gb/s NRZ signal's eye diagrams for the state of (b) free-running DFB LD2 (system I) and (c) DFB LD2 with an injection power of 3 dBm (system II).

with 3 dBm injection) [Fig. 7(b)] is around 5.1 dB lower than that detected by the PD (system I) [Fig. 7(a)]. This 5.1-dB amplitude penalty is mostly attributable to the responsivity lower than that of the PD [17]. As an injection-locked DFB LD2 functions as a PM-to-IM converter with an optical detector, its responsivity

is lower than that of the PD, thus lowering its amplitude output. As for the state of non-injection-locked DFB LD2 (system II; non-injection locking), no PAM4 signal is acquired [Fig. 7(c)] when the DFB LD2 has not injection-locked by the downstream optical signal.

The upstream BER performances of FSO communications with intensity-modulated 25-Gb/s NRZ signal in the scenarios over 600-m FSO link (system I) and that over 600-m FSO link (system II; with 3 dBm injection) are presented in Fig. 8(a). Contrary to the downstream BER performances [Fig. 6(a)], it is to be found that system II's upstream performance (with 3 dBm injection) is better than that of system I. With a 10^{-9} BER operation, a 2.1-dB power penalty emerges between systems II (with 3 dBm injection) and I. Given that the LD's chirp due to direct modulation is associated with the optical signal's phase deviation, a chirp reduction can be achieved by a LD with injection locking [35], [36]. A higher optical power injected into the DFB LD2 (3 dBm injection) will further suppress the DFB LD2's chirp in the upstream transmission, thus enhancing the upstream BER performance. As for NRZ eye diagrams, for the free-running DFB LD2 (system I), clear eye diagrams [Fig. 8(b)] are attained with a BER operation of 10^{-9} and a received optical power of -8.9 dBm. The DFB LD2 with an injection power of 3 dBm (system II) yields open eye diagrams [Fig. 8(c)], at a BER value of 10^{-9} and a received optical power of -11 dBm, due to the DFB LD2's chirp being effectively suppressed.

IV. CONCLUSION

A bidirectional FSO communication with downstream phase-modulated 25-Gb/s/25-GHz PAM4 passband signal and upstream intensity-modulated 25-Gb/s NRZ baseband signal through a 600-m free-space transmission is established. With optimal injection wavelength and injection power, a remotely injection-locked DFB LD is sufficient for a duplex transceiver. A DFB LD with remote injection locking not only operates as a PM-to-IM converter with an optical detector to detect the phase-modulated optical signal, but it also operates as an upstream optical carrier to provide better upstream performance. With the adoption of PM scheme and remotely injection-locked DFB LD, a satisfactorily low BER of 10^{-9} and clear PAM4/NRZ eye diagrams are acquired through a 600-m FSO link. This bidirectional FSO communication with a low-complexity duplex transceiver satisfies the need of high-speed FSO communication given its practicality for giving a two-way high-transmission-rate over a long-range free-space transmission. Such established bidirectional FSO communication opens up an innovative way for developing two-way high-speed optical wireless communications.

REFERENCES

- [1] I. Tomkos, D. Klionidis, E. Pikasis, S. Theodoridis, "Toward the 6G network era: Opportunities and challenges," *IEEE IT Professional*, vol. 22, no. 1, pp. 34–38, Jan.–Feb. 2020.
- [2] C. Y. Li, H. W. Wu, H. H. Lu, W. S. Tsai, S. E. Tsai, and J. Y. Xie, "A hybrid Internet/CATV/5G fiber-FSO integrated system with a triple-wavelength polarization multiplexing scenario," *IEEE Access*, vol. 7, pp. 151023–151033, Oct. 2019.
- [3] T. Kusunoki, T. Kurakake, K. Otsuki, and K. Saito, "Improvement of 4K/8K multi-channel IP multicast using DOCSIS over in-building coaxial cable network," in *Proc. IEEE Int. Conf. Consum. Electron.*, Jan. 2019, pp. 1–5.
- [4] M. Carmo, S. Jardim, A. Neto, R. Aguiar, D. Corujo, and J. J. P. C. Rodrigues, "Slicing WiFi WLAN-sharing access infrastructures to enhance ultra-dense 5G networking," in *Proc. IEEE Intl. Conf. Commun.*, May 2018, pp. 1–6.
- [5] F. Forni, N. C. Tran, H. P. A. van den Boom, E. Tangdiongga, and A. M. J. Koonen, "Simultaneous multiband WSN, WLAN, LTE-A, and Gb/s 4-PAM signals transmission over 50 m 1 mm core diameter POF for home area network," in *Proc. Opt. Fiber Commun. Conf.*, Mar. 2018, Paper Th2A.57.
- [6] A. E. Morra, K. Ahmed, and S. Hranilovic, "Impact of fiber nonlinearity on 5G backhauling via mixed FSO/fiber network," *IEEE Access*, vol. 5, pp. 19942–19950, Sep. 2017.
- [7] H. W. Wu *et al.*, "A 448-Gb/s PAM4 FSO communication with polarization-multiplexing injection-locked VCSELs through 600 m free-space link," *IEEE Access*, vol. 8, pp. 28859–28866, Feb. 2020.
- [8] K. Mallick, P. Mandal, R. Mukherjee, G. C. Mandal, B. Das, and A. S. Patra, "Generation of 40 GHz/80 GHz OFDM based MMW source and the OFDM-FSO transport system based on special fine tracking technology," *Opt. Fiber Technol.*, vol. 54, Jan. 2020, Art. no. 102130.
- [9] C. Abou-Rjeily, G. Kaddoum, and G. K. Karagiannidis, "Ground-to-air FSO communications: when high data rate communication meets efficient energy harvesting with simple designs," *Opt. Express*, vol. 27, no. 23, pp. 304079–304092, Nov. 2019.
- [10] K. Mallick, P. Mandal, G. C. Mandal, R. Mukherjee, B. Das, and A. S. Patra, "Hybrid MMW-over fiber/OFDM-FSO transmission system based on doublet lens scheme and POLMUX technique," *Opt. Fiber Technol.*, vol. 52, Nov. 2019, Art. no. 101942.
- [11] W. C. Wang, H. Y. Wang, and G. R. Lin, "Ultrahigh-speed violet laser diode based free-space optical communication beyond 25 Gbit/s," *Scientific Rep.*, vol. 8, Sep. 2018, Art. no. 13142.
- [12] G. C. Mandal, R. Mukherjee, B. Das, and A. S. Patra, "Next-generation bidirectional triple-play services using RSOA based WDM radio on free-space optics PON," *Opt. Commun.*, vol. 411, pp. 138–142, Mar. 2018.
- [13] J. Zhang *et al.*, "Fiber-wireless integrated mobile backhaul network based on a hybrid millimeter-wave and free-space-optics architecture with an adaptive diversity combining technique," *Opt. Lett.*, vol. 41, no. 9, pp. 1909–1912, May 2016.
- [14] H. Tian *et al.*, "Optical frequency comb noise spectra analysis using an asymmetric fiber delay line interferometer," *Opt. Express*, vol. 28, no. 7, pp. 9232–9243, Mar. 2020.
- [15] D. Fujimoto, H. H. Lu, K. Kumamoto, S. E. Tsai, Q. P. Huang, and J. Y. Xie, "Phase-modulated hybrid high-speed Internet/WiFi/Pre-5G in-building networks over SMF and PCF with GI-POF/IVLLC transport," *IEEE Access*, vol. 7, pp. 90620–90629, Jul. 2019.
- [16] C. Y. Chen *et al.*, "Bidirectional phased-modulated hybrid cable television/radio-over-fiber lightwave transport systems," *Opt. Lett.*, vol. 38, no. 4, pp. 404–406, Feb. 2013.
- [17] Q. Gu, W. Hofmann, M. C. Amann, and L. Chrostowski, "Optically injection-locked VCSEL as a duplex transmitter/receiver," *IEEE Photon. Technol. Lett.*, vol. 20, no. 7, pp. 463–465, Apr. 2008.
- [18] H. S. Su *et al.*, "Fiber optical CATV transport systems based on PM and light injection-locked DFB LD as a duplex transceiver," *Opt. Express*, vol. 19, no. 27, pp. 26928–26935, Dec. 2011.
- [19] C. Y. Li, X. H. Huang, H. H. Lu, Y. C. Huang, Q. P. Huang, and S. C. Tu, "A WDM PAM4 FSO-UWOC integrated system with a channel capacity of 100 Gb/s," *IEEE/OSA J. Light. Technol.*, vol. 38, no. 7, pp. 1766–1776, Apr. 2020.
- [20] Y. Pan, L. Yan, A. Yi, L. Jiang, W. Pan, and B. Luo, "Simultaneous demultiplexing of $2 \times$ PDM-PAM4 signals using simplified receiver," *Opt. Express*, vol. 27, no. 3, pp. 1869–1876, Feb. 2019.
- [21] G. W. Lu *et al.*, "Flexible generation of 28 Gbps PAM4 60 GHz/80 GHz radio over fiber signal by injection locking of direct multilevel modulated laser to spacing-tunable two-tone light," *Opt. Express*, vol. 26, no. 16, pp. 20603–20613, Aug. 2018.
- [22] W. S. Tsai, H. H. Lu, Y. C. Huang, S. C. Tu, and Q. P. Huang, "A PDM-based bi-directional fibre-FSO integration with two RSOAs scheme," *Scientific Rep.*, vol. 9, Jun. 2019, Art. no. 8317.
- [23] K. Mallick, R. Mukherjee, B. Das, G. C. Mandal, and A. S. Patra, "Bidirectional hybrid OFDM based wireless-over-fiber transport system using reflective semiconductor amplifier and polarization multiplexing technique," *Int. J. Electron. Common. (AEÜ)*, vol. 96, pp. 260–266, Nov. 2018.
- [24] S. M. Jung, S. K. H. Mun, M. Kang, and S. K. Han, "Optical signal suppression by a cascaded SOA/RSOA for wavelength reusing reflective PON upstream transmission," *Opt. Express*, vol. 25, no. 19, pp. 22851–22858, Sep. 2017.
- [25] S. Mhatli *et al.*, "Long-reach OFDM WDM-PON delivering 100Gb/s of data downstream and 2Gb/s of data upstream using a continuous-wave laser and a reflective semiconductor optical amplifier," *Opt. Lett.* vol. 39, pp. 6711–6714, Dec. 2014.

- [26] H. H. Lu *et al.*, "Bidirectional fiber-IVLLC and fiber-wireless convergence system with two orthogonally polarized optical sidebands," *Opt. Express*, vol. 25, no. 9, pp. 9743–9754, May 2017.
- [27] K. Y. Cho, Y. Takushima, and Y. C. Chung, "10-Gb/s operation of RSOA for WDM-PON," *IEEE Photon. Technol. Lett.*, vol. 20, no. 18, pp. 1533–1535, Sep. 2008.
- [28] S. Mohrdiek, H. Burkhard, and H. Walter, "Chirp reduction of directly modulated semiconductor lasers at 10 Gb/s by strong CW light injection," *IEEE/OSA J. Light. Technol.*, vol. 12, no. 3, pp. 418–424, Mar. 1994.
- [29] H. Kaushal and G. Kaddoum, "Optical communication in space: challenges and mitigation techniques," *IEEE Commun. Surveys Tuts.*, vol. 19, no. 1, pp. 57–96, Jan–Mar. 2017.
- [30] K. Mallick, P. Mandal, G. C. Mandal, R. Mukherjee, B. Das, and A. S. Patra, "Hybrid MMW-over fiber/OFDM-FSO transmission system based on doublet lens scheme and POLMUX technique," *Opt. Fiber Technol.*, vol. 52, Nov. 2019, Art. no. 101942.
- [31] H. H. Lu *et al.*, "64 Gb/s PAM4 VCSEL-based FSO link," *Opt. Express*, vol. 25, no. 5, pp. 5749–5757, Mar. 2017.
- [32] P. Saboureau, J. P. Foing, and P. Schanne, "Injection-locked semiconductor lasers with delayed optoelectronic feedback," *IEEE J. Quantum Electron.*, vol. 33, no. 9, pp. 1582–1591, Sep. 1997.
- [33] I. I. Kim, B. McArthur, and E. Korevaar, "Comparison of laser beam propagation at 785 nm and 1550 nm in fog and haze for optical wireless communications," *Proc. SPIE*, vol. 4214, pp. 26–37, Feb. 2001.
- [34] S. Wiczorek, W. W. Chow, L. Chrostowski, and C. J. C. Hasnain, "Improved semiconductor-laser dynamics from induced population pulsation," *IEEE J. Sel. Topics Quantum Electron.*, vol. 42, no. 6, pp. 552–562, Jun. 2006.
- [35] Y. C. Lee, C. T. Tsai, Y. C. Chi, Y. H. Lin, and G. R. Lin, "Chirp manipulation of harmonically mode-locked weak-resonant-cavity colorless laser diode with external fiber ring," *IEEE J. Quantum Electron.*, vol. 51, no. 2, Feb. 2015, Art. no. 1300111.
- [36] G. Yabre, "Effect of relatively strong light injection on the chirp-to-power ratio and the 3 dB bandwidth of directly modulated semiconductor lasers," *IEEE/OSA J. Light. Technol.*, vol. 14, no. 10, pp. 2367–2373, Oct. 1996.

Xu-Hong Huang received the MS degree from the College of Physics and Information Engineering, Fuzhou University, China, in 2003. She joined Fujian Hitachi TV as an Engineer in 1990 and was promoted to Senior Engineer in 2000. She joined the School of Information Science and Engineering, Fujian University of Technology as an Associate Professor, in 2003. Her research interests include FSO communications, UWOC systems, and FSO-UWOC integration. She has authored or co-authored more than 25 papers in SCI-cited international journals and more than eight papers in international conferences. Associate Professor Huang is currently a Fellow of the Fujian Electronics Society and a Fellow of the Fujian Electrical Engineering Society. She was awarded with the Fujian Superior New Product Award (1995, 1996, and 1998), the National Education Research Institute Excellent Paper Award (2009), and the Utility Model Invention Award (2013 and 2014).

Chung-Yi Li received his MS and PhD degrees from the Department of Electro-Optical Engineering, National Taipei University of Technology (NTUT), Taiwan, in 2008 and 2012, respectively. From 2013 to 2014, he was an Engineer with the Innovation and Product Development Department, FOCI Fiber Optic Communications, Inc., Hsinchu, Taiwan. He joined the Department of Electro-Optical Engineering at NTUT as a Research Assistant Professor, in 2014. He joined the Department of Communication Engineering, National Taipei University as an Assistant Professor, in 2018. His research interests include FSO communications, UWOC systems, and FSO-UWOC integration.

Hai-Han Lu (Senior Member, IEEE) received the MS and PhD degrees from the Institute of Optical Science, National Central University, Taiwan, in 1991 and 2000, respectively. He joined the Department of Electro-Optical Engineering at National Taipei University of Technology (NTUT) as an Associate Professor in 2003. He was promoted to a Professor, Distinguished Professor, and Lifetime Distinguished Professor in 2003, 2006, and 2017, respectively. His research interests include FSO communications, fiber-FSO convergence, UWOC systems, and FSO-UWOC integration. He has authored or co-authored more than 200 papers in SCI-cited international journals and more than 130 papers in international conferences. Professor Lu is currently a Fellow of SPIE, a Fellow of IET, a Senior Member of IEEE, and a Senior Member of OSA. He was awarded with the Sun Yat-Sen Academic Award (Natural Science, 2017), National Invention Award (Gold Medal, 2016), ICT Month Innovative Elite Products Award (2014 and 2016), Outstanding Electrical Engineering Professor Award of the Chinese Institute of Engineering (2015), Outstanding Engineering Professor Award of the Chinese Engineer Association (2013), and Outstanding Research Award of NTUT (2004) for his significant technical contributions to FSO communications, fiber-FSO convergence, UWOC systems, and FSO-UWOC integration.

Cing-Ru Chou was born in Taoyuan city, Taiwan, in June 1997. He received the BS degree from Yuan Ze University, Taoyuan, Taiwan, in 2019. He is currently working toward the MS degree with the Institute of Electro-Optical Engineering, National Taipei University of Technology, Taiwan. His research interests focus on FSO communications and UWOC systems.

Hsin-Mao Hsia was born in Hsinchu, Taiwan, in November 1995. He received the BS degree from Tunghai University, Taichung, Taiwan, in 2019. He is currently working toward the MS degree with the Institute of Electro-Optical Engineering, National Taipei University of Technology, Taiwan. His research interests focus on FSO communications and UWOC systems.

Yi-Hao Chen was born in Changhua County, Taiwan, in March 1997. He received the BS degree from the National Yunlin University of Science and Technology, Yunlin County, Taiwan, in 2019. He is currently working toward the MS degree with the Institute of Electro-Optical Engineering, National Taipei University of Technology, Taiwan. His research interests focus on FSO communications and UWOC systems.